

Doughnut shape atom traps with arbitrary inclination

R. Rodríguez y Masegosa^{a,b}, H. Moya-Cessa^a, and S. Chávez-Cerda^a

^a INAOE, Apartado Postal 51 y 216, 72000 Puebla, Pue. Mexico

^b Photonics and Mathematical Optics Group, Tecnológico de Monterrey, Garza Sada 2501, Monterrey, N.L., Mexico 64849

Recibido el 16 de junio de 2005; aceptado el 31 de octubre de 2005

Since the invention of magneto-optical trap (MOT), there have been several experimental and theoretical studies of the density distribution in these devices. To the best of our knowledge, only horizontal orbital traps have been observed, perpendicular to the coil axis. In this work we report the observation of distributions of trapped atoms in pure circular orbits without a nucleus whose orbital plane is tilted up to 90° with respect to the horizontal plane. We have used a stabilized time phase optical array in our experiments and conventional equipment used for MOT.

Keywords: Atom traps; atom cooling; Bose Einstein condensates; atom guides; magneto-optical traps; radiation pressure; orbital angular moment.

Desde la invención de la trampa magneto-óptica (TMO), ha habido varios estudios teóricos y experimentales sobre la distribución de densidad en tales dispositivos. Las distribuciones logradas han sido solo en forma horizontal, perpendiculares con respecto del eje de la bobina. En este trabajo, reportamos la observación de distribuciones de trampas atómicas en órbitas circulares sin núcleo cuyo plano orbital es inclinado hasta 90° con respecto del plano horizontal. Hemos usado en nuestros experimentos un arreglo de fase óptica estabilizado en tiempo y equipo convencional usado en trampas magneto-ópticas.

Descriptores: Trampas atómicas; condensación Bose Einstein; guías atómicas; trampas magneto-ópticas; presión de radiación; momento angular orbital.

PACS: 32.80.-t; 32.80.Lg; 32.80.PJ

1. Introduction

Cooling and trapping atoms, using radiation pressure force, has been studied extensively in the past few years [1, 2]. Initial works in this field aimed at controlling atom beam paths [3, 4], originating what are known as atom guides [5]. Later works reported reducing the speed of atoms by means of laser beams, allowing for a better control of atom guides. This led to a new research area known as atom cooling. Gas or atom cooling, using three pairs of counter-propagating laser beams crossing at a region in space, was proposed initially in 1975 [1] and it is the most used configuration in atom trapping. With the first atom traps, it was possible to achieve atom confinements at temperatures of the order of μK [2]. Currently, the lowest temperatures that have been reached are of the order of nK , making it possible to obtain Bose-Einstein condensates. The behaviour of cold atoms in various trap configurations (magnetic traps, dipolar traps, magneto-optical traps, for instance) have been studied and allow us to explain several effects observed those traps such as collisions [6], loading time rate [7], spring constant and temperature [8], and trap shapes [10].

A special topic of laser cooling that has received much attention is the formation of spatial atomic distributions [11, 12]. One particular case, ever since it was observed for the first time (1990), is that of the “doughnut shaped trap” or “ring shaped trap” distributions [9, 10].

Even though the doughnut shaped traps have been studied extensively [13–20], there is a limit of 20 degrees of inclination reported by Sesko *et al.* that has not been questioned or

treated in later papers that analyze the formation of orbital traps.

These distributions have been explained as an orbital motion of the atoms induced by the trapping beams, where a small misalignment of the beams directed at the atoms in opposite directions is such that they create a torque in the cloud of atoms [9]. Sesko *et al.* [10] have tried to explain some of the mechanics involved in the generation of ring shapes. The misalignment done was called “racetrack geometry” by Arnold and Manson [21]. It causes a torque on the atom cloud, generating an angular momentum and consequently the formation of a ring of atoms. There have also been theoretical studies that simulate such distributions in optical molasses by Castin and Molmer [22]. In their simulations, a constant phase difference between the counter-propagating beams was considered. In their work, they predicted in their work orbital traps at an angle equal to 45° to the horizontal plane.

Related to these distributions of trapped atoms, there are also some special cases in which the atom clouds take three dimensional forms with spherical symmetry. These distributions are controlled by a slight misalignment of the optical array in combination with the control of the magnetic field gradient. For example, there have been reports on the observation of clouds of atoms moving in an orbital shape around a nucleus of trapped atoms, and this nucleus is always present at the trap center [9]; also reported was the observation of ring-shaped traps without a central nucleus [10, 17]. Besides the previous forms of traps there have been other

works reporting more complicated structures such as double rings [16].

Walker *et al.* [9] and Sesko *et al.* [10] observed that the ring shape traps have unstable orbital motion for inclinations greater than 20° , the horizontal plane being perpendicular to the axis of the solenoid. Sesko *et al.* explained that this instability is due to the different magnetic gradients along the horizontal plane and vertical axis where the confinement force is

$$F_{spring} = -k_{spring}(x, y, 2z). \quad (1)$$

In this contribution, we report the experimental generation of stable magneto-optical traps (MOT) with a doughnut shape whose orbital plane may have inclinations of up to 90° . The misalignment needed to observe this effect is smaller than those reported previously in the literature [10]. Our experimental observations agree qualitatively with the theoretical predictions of Castin and Molmer [22], because in the experimental setup we have kept the relative phase constant between the six beams, which was imposed as a condition to obtain doughnut shaped traps at about 45 degrees [22].

2. Experimental apparatus

For trapping ^{85}Rb atoms from a vapor gas, we have employed the standard configuration of an MOT, *i.e.* three pairs of appropriately circularly polarized, counter propagating laser beams intersecting at the centre of the magnetic quadrupole field that is created by two coils with opposite electric currents (Fig. 1). To produce rubidium atoms in our experiments, we have used a getter that allows a controlled dosage of atoms; therefore is not necessary to use a shutter as is usually done with ovens [7, 24]. In Fig. 2, the scaled dimensions of the vacuum system are shown. The distance from the getter to the centre of the vacuum camera is 135 mm, which is a short distance compared to the minimum stop distance that is obtained when the atoms are produced in an oven (750 mm for rubidium at 1 Torr pressure) [25].

In order to calculate the number of trapped atoms, we measured the fluorescence of the atomic cloud; we used a photo-multiplier that was protected with a transmission filter at 780 nm. We estimated the trap dimensions analyzing the images obtained with a CCD camera previously calibrated to estimate the atom density (atoms/m³).

With respect to the trap beam alignment, typical arrays in MOT use two beam splitters to produce the beams for each dimension (x, y, z). The experimental array that we have used is shown in Fig. 2, where it should be noticed that we are using only one beam splitter (its advantage will be explained below).

The trapping laser is linearly polarized and enters from the right as shown in Fig. 2, passing through the $\lambda/4$ retarder and emerging as a circular polarized beam that is split with a polarizer cube. Rotating this first $\lambda/4$ retarder, we can adjust the intensity of the two orthogonal linearly polarized beams that emerge from the cube. The other $\lambda/4$ retarders produce

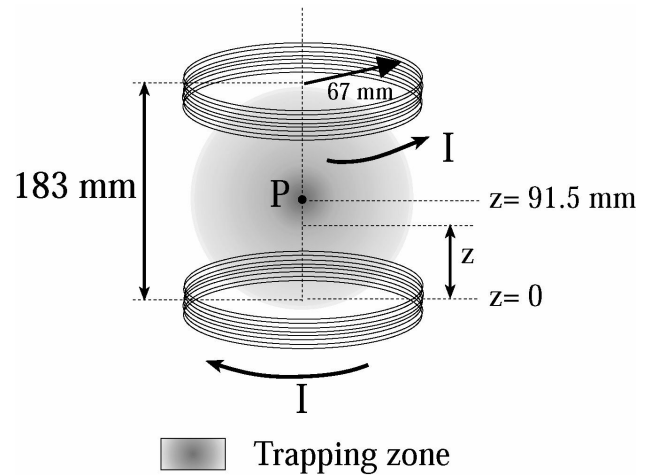


FIGURE 1. Coil array for magnetic gradient generation. In this picture the dimensions that we have chosen are showed.

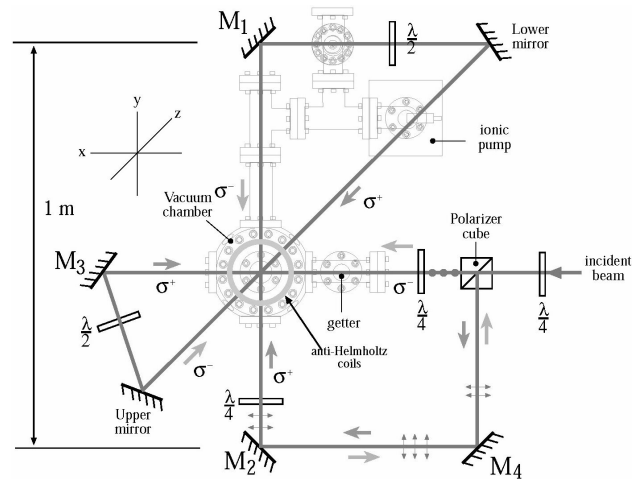


FIGURE 2. Optical array implemented in our experiments. The $\lambda/4$ retarders change the linear polarization to circular polarization, while the $\lambda/2$ retarders correct the polarization after some reflections.

circular polarized beams and are adjusted to make them mutually orthogonal, denoted as σ^+ and σ^- in Fig. 2. The $\lambda/2$ retarders make a correction of circularity in the polarization caused by the first reflections. The alignment of laser beams was done in three dimensions as is shown in Fig. 2. In this optical array, we can see the strong dependence on the six trapping beams; any movement or vibration in one mirror affects the whole system. In fact, a basic feature of this optical array is the constant relative (time) phase that exists between counter-propagating beams because of the fact that we used only one polarization cube to obtain all beams in combination with six mirrors [26, 27].

The atoms emitted by the dispenser entered the vacuum chamber with the ion pump was working at all times. The nominal operation of the dispenser at $I_{th} = 3.2$ A, which produced a constant pressure of 3×10^{-10} Torr, similar to Ref. 7.

We have used diode lasers as the trapping and pump beams. Light from a diode laser drives the $5S_{1/2}(F=3) \rightarrow 5P_{3/2}(F'=4)$ transition in ^{85}Rb (natural linewidth $\Gamma/2\pi = 5.98$ MHz) at a wavelength of 780 nm with a total peak intensity of 12 mW/cm^2 .

To provide hyperfine pumping, we launched a second laser beam to re-pump the atoms on the $5S_{1/2}(F=2) \rightarrow 5P_{1/2}(F'=3)$ transition.

The control laser for frequency lock-in was made using a saturation absorption spectroscopy array and monitoring the signal from the sensors to control a piezoelectric that, in the Littrow configuration, is responsible for laser tuning.

To stabilize the laser operation, it was necessary to control the temperature with a precision of 0.01°C and the electric current with a $10\mu\text{A}$ precision. By controlling these parameters, stable operation in the trap was observed in periods of time of up to 15 minutes depending on environmental conditions. The trapping laser was set to mono-mode operation and its stabilization was protected with an optical isolator. The optical isolator function is to avoid feedback effects the stability of the laser. The laser diode emission pattern has an elliptic transverse distribution (1:4 in our experiment), and this can increase losses in the spatial filter. Moreover, this distribution of energy can affect the trap uniformity, and it must be spherical when the optical array alignment is optimized. To correct this, and to produce a circular Gaussian beam, we employed a pair of anamorphic prisms to reduce the elliptic distribution (emitted by the diode laser) by a factor of three.

To obtain a magnetic field gradient of the MOT, we used two solenoids with electric counter-currents. The solenoid dimensions were 14 cm in diameter separated by 18 cm, and the beam alignment was made to intersect at the point where the magnetic field is zero. The vertical magnetic field gradient could vary from 0 to 6.5 G/cm .

3. Results

We first checked the optical alignment before obtaining orbital traps. A uniform spherical distribution cloud is trapped in the MOT; we then expanded and compressed the cloud by changing the magnetic gradient or detuning, observing that the trap remained in the same spatial point.

To simplify our experimental setup, we did not use additional coils to center the zero magnetic field on the beams' intersection [9, 10]. Instead we adjusted the beam alignment at the point where the magnetic field was zero. The only disadvantage that we found was that the mirrors must be tilted until a perfect alignment is obtain.

As we have mentioned before, the orbital trap is formed by making a little misalignment in the optical array, causing a torque to the cloud of trapped atoms. The misalignment in our case was smaller than 1 mrad with respect to the optimal position, and it was made by tilting the mirror $M1$ (see Fig. 2) and adjusting the upper mirror to obtain a uniform

orbital pattern. As we moved the mirror $M1$, the doughnut-shaped cloud was oriented in the reference frame as shown in the inset of Fig. 3. Also, in Fig. 3, the observation windows are shown where two video cameras were placed to capture the two perpendicular views (MW1 and MW2) from the atom trap.

The number of atoms was estimated in 3.3×10^6 and the averages densities were $2.9 \times 10^{11} \text{ atoms/cm}^3$. The charge time did not show variation for any condition of orbital motion. The loading time was the same for all orbital traps studied, regardless of the inclination. Fig. 4 shows the characteristic loading time of the orbital traps, where the constant time was $\tau=1.257 \text{ s}$. We estimated that signal oscillations are of the order of 5% variation, indicating an excellent stability of the traps formed.

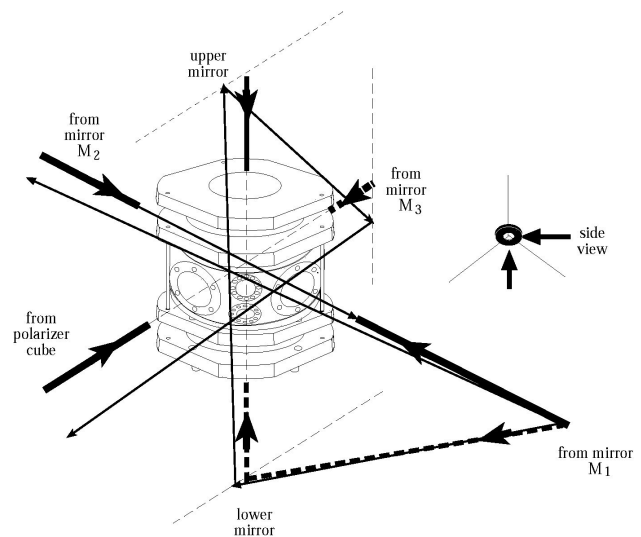


FIGURE 3. Misalignment of laser beams to obtain orbital traps. The frontal view was observed in window 1 (MW1), and the lateral view was observed in mirror 2 (MW2). The doughnut orientation was as shown in this picture. The dashed lines show the alignment path and solid blue lines indicate the new misalignment path. The red solid lines are path unchanged. The inset shows the exact orientation of doughnuts as indicated in the pictures with captions frontal and lateral views.

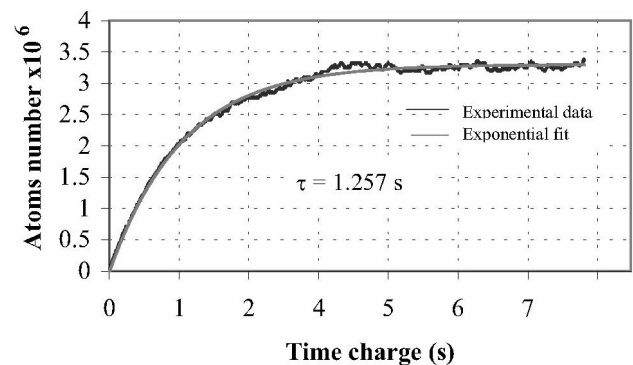


FIGURE 4. Number of trapped atoms in a doughnut shape configuration as a function of the loading time.

The magnetic field gradient was the main parameter that affected the orbital features, namely ratio and the number of trapped atoms. We observed that the difference between the magnetic field gradients in the $x - y$ plane and the z axis did not affect the stability trap.

Following Sesko *et al.* [10], the frequency detuning of the trapping laser was fixed in 10 Mhz and it did not show significant effects on the orbital dimensions. However changes in the fluorescence were observed that are related to the number of trapped atoms. The detuning was fixed so that a maximal fluorescence was obtained, indicating the maximum number of trapped atoms.

Figures 5a and 5b show two photographic sequences that were obtained at the two windows as shown in Fig. 2. In Figs. 5a and 5b is shown a photographic sequence for the atom trap as a function for the magnetic field gradient. Different mirror misalignment was used for Figs. 5a and 5b, producing different tilt angles of the orbital plane of the atom traps. For Fig. 5a, an inclination of 45° was estimated with respect to the horizontal plane, while for Fig. 5b the angle was about 80° . The dependence of the trap dimension versus magnetic field gradient is shown in Fig. 6.

To estimate the dimensions of the trap (shown in Fig. 6), we fitted the distributions of the doughnut trap at 45° with a Laguerre-Gaussian function. We can observe the linear behaviour in the inner diameter as well as the outer diameter as a function of the magnetic field gradient. When they intersect, the trap distribution changes from a doughnut shape to a spherical shape. This occurs for a magnetic field of the order of 4.13 G/cm. An interesting fact is that, by reducing the field again, the doughnut shape is recovered.

Finally, we obtained a trap with an orbital motion plane parallel to the solenoid's axis (perpendicular to horizontal plane $x-y$). Figure 7 shows the two orthogonal views of this extreme case, where we can see the circular symmetry due to the perspective captured by the video camera. The equation that we have used in this fitting to calculate the trap dimensions is:

$$y = y_0 + \frac{\bar{A}}{\bar{\omega}\sqrt{\pi/2}} e^{-2\frac{(x-x_{c1})^2}{\bar{\omega}^2}} + \frac{\bar{A}}{\bar{\omega}\sqrt{\pi/2}} e^{-2\frac{(x-x_{c2})^2}{\bar{\omega}^2}}, \quad (2)$$

where y is the intensity level related to x (pixel) position, y_0 is an adjusting parameter, $\bar{\omega}$ is the average width of the doughnut using Gaussian functions fit, x_{c1} and x_{c2} are the central points of each Gaussian function. As we mentioned before, the fit for the diameter calculation of doughnut-shapes was made with the intersection of two Gaussian functions represented by Eq. (2) and that is shown in Fig. 8. The estimate in this case for the external diameter was 1.193 mm and 0.57 mm for the inner diameter (hole diameter). The magnetic gradient was 2.48 G/cm for this same situation. The orbital traps observed in all situations, including this case, were very stables (< 5 min) depending only on the frequency lock-in stability of the trapping and pumping lasers.

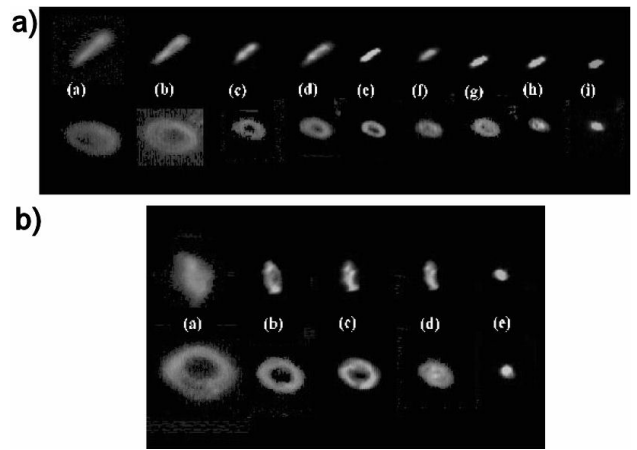


FIGURE 5. Orbital trap sequence, where the angle was (a) 45° with respect to the horizontal axis or 45° with respect to the coil axes, (b) 80° with respect to the horizontal axis or 10° with respect to coil axes. The control parameter was the magnetic field gradient for each sequence.

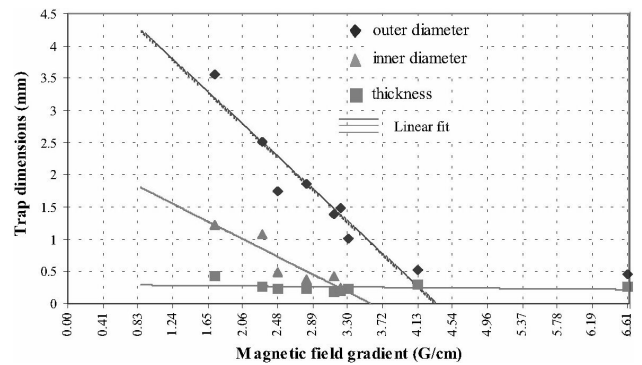


FIGURE 6. Diameter variation from orbital traps at an inclination 45° . This linear behavior was present in all cases of orbital plane inclination.

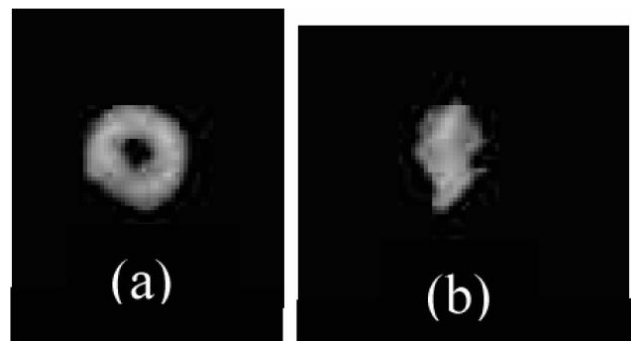


FIGURE 7. Orbital trap at 90° with respect to the horizontal plane or 0° with respect to the coil axis. In Fig. 7a is showed the frontal view captured from MW1 shown in Fig. 3. In Fig. 7b is showed the lateral view captured from MW2 shown in Fig. 3.

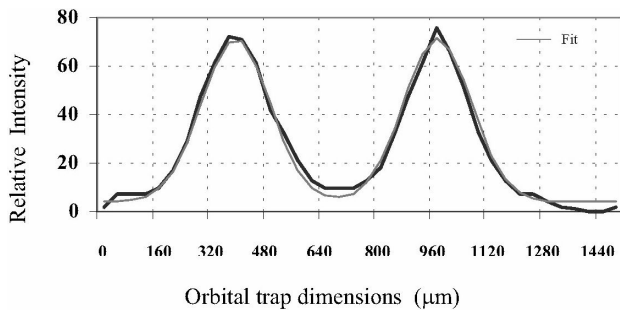


FIGURE 8. Doughnut fit to two Gaussians functions for diameter estimation (we have used Eq. 2).

4. Conclusions

We have observed stable orbital traps (OT) at angles greater than 20° with respect to the horizontal plane. The stability of the traps depends only on the frequency lock-in and the thermal and mechanical variations of the mirror's mounts. The difference between the magnetic field gradients in the

x-y plane and vertical axis z is not a problem in obtaining orbital traps at angles greater than 20° . Stable OT at 45° were predicted with stable phase condition in a simulation by Castin and Molmer; in this work we have experimentally demonstrated them. By changing the detuning we observed changes in fluorescence emitted by atoms trapped (therefore a increase or decrease of trapped atoms), but we do not have observed changes in OT dimensions. However, the variation of the magnetic field gradient strongly affected the dimensions of the OT, and a linear dependence of the internal and external diameters was found. When these diameters are equal to the width of the distribution, the geometry of the trap goes to an spherical one.

The behaviour of the diameter hole is almost linear, so that it only exists in a magnetic gradient range. In addition, we can obtain the OT at any angle with respect to vertical axis, varying only the alignment of the optical array. Finally, to obtain these results, missalignment was < 1 mrad with respect to the optimal alignment, and this is smaller than that reported in the literature.

1. T.W. Hänsch and A.L. Schawlow, *Opt. Comm.* **13** (1975) 68.
2. A. Ashkin, *Phys. Rev. Lett.* **40** (1978) 729.
3. J.E. Bjorkholm, R.R. Freeman, A. Ashkin, and D.B. Pearson, *Phys. Rev. Lett.* **41** (1978) 1361.
4. A. Ashkin, *Phys. Rev. Lett.* **25** (1970) 1321.
5. K. Dholakia, *Contemporary Physics* **39** (1998) 351.
6. D. Sesko, T. Walker, C. Monroe, A. Gallagher, and C. Wieman, *Phys. Rev. Lett.* **63** (1989) 961.
7. Umakant D. Rapol, Ajay Wasan, and Vasant Natarajan, *Phys. Rev. A* **64** (2001) 23402.
8. C.D. Wallace *et al.*, *J. Soc. Am. B* **050703** (1994) 703.
9. T. Walker, D. Sesko, and C. Wieman, *Phys. Rev. Lett.* **64** (1990) 408.
10. D.W. Sesko, T.G. Walker, and C.E. Wieman, *J. OPT. SOC. AM. B* **8** (1991) 946.
11. S. Peil *et al.*, *Phys. Rev. A* **8** (2003) 051603(R).
12. L. Guidoni and P. Verkerk, *J. Opt. B* **1** (1999) R23.
13. V.S. Bagnato *et al.*, *Phys. Rev. A* **48** (1995) 3771.
14. M.T. de Araujo *et al.*, *Opt. Comm.* **119** (1995) 85.
15. F. Dias Nunes, J.F. Silva, S.C. Zilio, and V.S. Bagnato, *Phys. Rev. A* **54** (1996) 2271.
16. D. Felinto, L.G. Marcassa, V.S. Bagnato, S.S. Vianna, *Phys. Rev. A* **60** (1999) 2591.
17. I. Guedes *et al.*, *J. Opt. Soc. Am. B* **11** (1994) 1935.
18. D. Felinto, and S.S. Vianna, *J. Opt. Soc. Am. B* **17** (2000).
19. D. Felinto, H. Regehr, J.W.R. Tabosa, and S.S. Vianna, *J. Opt. Soc. Am. B* **18** (2001).
20. Reinaldo L. Cavasso Filho *et al.*, *Brazilian J. Phys.* **33** (2003).
21. A.S. Arnold and P.J. Manson, *J. Opt. Soc. Am. B* **17** (2000) 497.
22. Yvan Castin and Klaus Molmer, *Phys. Rev. Lett.* **74** (1995) 3772.
23. R.N. Watts and C.E. Wieman, *Opt. Lett.* **11** (1986) 291.
24. J. Fortagh, A. Grossmann, T.W. Hänsch, and C. Zimmermann, "Fast loading of magneto-optical trap from a pulsed thermal source", **84** (1998) 6499.
25. Harold J. Metcalf, Peter van der Straten, "Laser Cooling and Trapping" (Springer, 1999).
26. A. Rauschenbeutel, H. Schadwinkel, V. Gomer, and D. Meschede, *Opt. Comm.* **148** (1998) 45.
27. Stephen Dale G. , Ph. D. Thesis, University of Connecticut, 1994.